

## Deviations from Kleinman symmetry measured for several simple atoms and molecules

Victor Mizrahi and D. P. Shelton

*Department of Physics, University of Toronto, Toronto, Ontario, Canada M5S 1A7*

(Received 17 December 1984)

Deviations from Kleinman symmetry for the second hyperpolarizability tensors of some simple atoms and molecules (He, Ar, Kr, Xe, CH<sub>4</sub>, CF<sub>4</sub>, SF<sub>6</sub>, H<sub>2</sub>, D<sub>2</sub>, N<sub>2</sub>, O<sub>2</sub>, CO<sub>2</sub>, C<sub>2</sub>H<sub>6</sub>, CHF<sub>3</sub>, and C<sub>2</sub>H<sub>4</sub>) have been measured down to the 0.1% level of accuracy at several frequencies far below the first strong electronic resonance, by means of dc-electric-field-induced second-harmonic generation (ESHG). The results of the experiment are discussed within the framework of several models. The observed Kleinman-symmetry deviations are small compared to the electronic dispersion, and appear to be dominated by electronic rather than vibrational contributions. However, vibrations are shown to play a role in the case of H<sub>2</sub>, and the results observed for H<sub>2</sub> and D<sub>2</sub> differ significantly. The observed deviation for He is relatively large and should provide a sensitive test of *ab initio* calculations.

### I. INTRODUCTION

Nonlinear optics has become a well-established means of studying the properties of matter.<sup>1,2</sup> Nonlinear optical processes are mediated by the nonlinear susceptibilities, which in general are tensors whose components are a function of the frequencies of the applied fields.<sup>3</sup> The nonlinear susceptibilities are subject to a number of symmetries dependent upon the nature of the experiment and the underlying symmetry of the system.<sup>4</sup> Some time ago, in an attempt to elucidate the nature of the mechanism chiefly responsible for second-harmonic generation in ionic crystals, it was proposed by Kleinman that high-frequency electronic processes lying well above the optical frequencies employed ( $\omega \sim 10^4$  cm<sup>-1</sup>) could be well represented by nonlinear susceptibilities totally symmetric in their spatial indices.<sup>5</sup> This is now referred to as Kleinman's conjecture<sup>6,7</sup> or Kleinman symmetry.<sup>8</sup> However, for ionic processes lying below the optical frequencies employed, such a symmetry was deemed inappropriate. Therefore, by studying the symmetry properties of the nonlinear susceptibility tensor it was suggested that the dominant contributing mechanism could be identified.

Accurate tests of Kleinman's conjecture in solids have proven difficult, although some results are available.<sup>9,10</sup> In gases the most accurate test so far reported has been made in inert-gas systems.<sup>11</sup> These measurements, made at  $\lambda = 694.3$  nm, showed no significant departure from Kleinman symmetry at the 1% level of accuracy. Since there can only be electronic processes operative in such systems, the results give a measure of the validity of the conjecture. However, measurements of comparable accuracy made for some molecules indicate small deviations from Kleinman symmetry.<sup>12,13</sup> It can be asked whether the analog of Kleinman's original program, when applied to gaseous media, might not prove a sensitive means of distinguishing between vibrational and electronic contributions to nonlinear processes in molecules.

In the following section we will review the theory and establish notation. In Sec. III we give details of the dc-

electric-field-induced second-harmonic generation (ESHG) experiment used to test for departures from Kleinman symmetry down to the 0.1% level for a variety of atoms and molecules at several wavelengths. In Sec. IV we present the results of the experiment and in Sec. V we discuss the results within the framework of several models and calculate the vibrational contribution in H<sub>2</sub>. Finally in Sec. VI we summarize the essential conclusions.

### II. THEORY

In our experiment we are concerned with the process of electric-field-induced second-harmonic generation (ESHG) in gases for which, following the notation of Bogaard and Orr,<sup>3</sup> we have

$$\mu_\alpha(2\omega) = \frac{1}{4} \gamma_{\alpha\beta\gamma\delta}(-2\omega; \omega, \omega, 0) E_\beta(\omega) E_\gamma(\omega) E_\delta(0), \quad (1)$$

where  $E_\beta(\omega)$  is the  $\beta$  spatial component in the molecular frame of the applied field oscillating at frequency  $\omega$ ,  $\mu_\alpha(2\omega)$  is the  $\alpha$  component of the induced dipole moment, and  $\gamma_{\alpha\beta\gamma\delta}(-2\omega; \omega, \omega, 0)$ , a fourth-rank Cartesian tensor, is the second hyperpolarizability tensor. Summation over repeated indices is implied.

The hyperpolarizabilities possess a number of symmetry properties.<sup>3,4,8,14,15</sup> Kleinman symmetry is the assumption that the hyperpolarizabilities are invariant under any permutation of their spatial indices. Since this invariance can be shown to be exact in the static limit,<sup>8,15</sup> and therefore in the limit of zero dispersion, it is tempting to apply Kleinman symmetry more generally, especially since doing so results in a significant reduction in the number of independent components of the hyperpolarizabilities.

The macroscopic analog of Eq. (1) is

$$P_i(2\omega) = \frac{3}{2} \chi_{ijkl}^{(3)}(-2\omega; \omega, \omega, 0) E_j(\omega) E_k(\omega) E_l(0), \quad (2)$$

where  $E_j(\omega)$  is now the  $j$ th component (in the laboratory frame) of the macroscopic applied field,  $P_i(2\omega)$  is the induced macroscopic polarization oscillating at  $2\omega$ , and  $\chi^{(3)}$  is the third-order nonlinear susceptibility, which for a gas

is related to  $\gamma$  by

$$\chi^{(3)} = \frac{1}{6} \rho L \langle \gamma \rangle, \quad (3)$$

where  $\rho$  is the number density of the molecules and the angular brackets signify an isotropic average.  $L$  represents the local-field correction factor, which in fact may be neglected for our purposes.

Since  $\chi^{(3)}$  is an isotropic tensor, it has at most only three independent elements,<sup>16</sup> and we may write<sup>17</sup>

$$\begin{aligned} \chi_{zzz}^{(3)}(-2\omega; \omega, \omega, 0) &= \chi_{zzz}^{(3)}(-2\omega; \omega, \omega, 0) \\ &+ \chi_{zxx}^{(3)}(-2\omega; \omega, \omega, 0) \\ &+ \chi_{zzx}^{(3)}(-2\omega; \omega, \omega, 0). \end{aligned} \quad (4)$$

A further simplification is possible. It follows from the definition of the hyperpolarizabilities (and their macroscopic analog) that we may, without loss of generality, construct them so as to be invariant under a simultaneous interchange of the field frequency arguments together with their corresponding spatial indices, but not including the polarization frequency and its spatial index.<sup>4</sup> Following Butcher we will refer to this as intrinsic permutation symmetry. For ESHG intrinsic permutation symmetry reduces the number of independent components of  $\chi_{ijkl}^{(3)}(-2\omega; \omega, \omega, 0)$  to two.

Let us define<sup>11</sup>

$$R(\omega) \equiv \chi_{zzz}^{(3)}(-2\omega; \omega, \omega, 0) / \chi_{zxx}^{(3)}(-2\omega; \omega, \omega, 0). \quad (5)$$

Intrinsic permutation symmetry applied to Eq. (4) yields

$$\begin{aligned} \gamma_{\alpha\beta\gamma\delta}(-\omega_\sigma; \omega_1, \omega_2, \omega_3) &= (1/\hbar^3) \sum_P \left[ \sum_{m,n,p (\neq g)} \frac{\langle g | \mu_\alpha | m \rangle \langle m | \mu_\delta | n \rangle \langle n | \mu_\gamma | p \rangle \langle p | \mu_\beta | g \rangle}{(\omega_{mg} - \omega_\sigma)(\omega_{ng} - \omega_1 - \omega_2)(\omega_{pg} - \omega_1)} \right. \\ &\quad \left. - \sum_{m,n (\neq g)} \frac{\langle g | \mu_\alpha | m \rangle \langle m | \mu_\delta | g \rangle \langle g | \mu_\gamma | n \rangle \langle n | \mu_\beta | g \rangle}{(\omega_{mg} - \omega_\sigma)(\omega_{ng} - \omega_1)(\omega_{ng} + \omega_2)} \right], \end{aligned} \quad (9)$$

where  $\sum_P$  implies a summation over all of the terms generated by permuting the frequencies with their associated spatial subscripts,  $\omega_\sigma = \omega_1 + \omega_2 + \omega_3$ , and  $\mu_\alpha$  is the  $\alpha$  component of the electric dipole moment operator.

For field frequencies below the lowest resonant frequency of the system we may perform a power series expansion about the origin, writing an expression of the form

$$\gamma(-2\omega; \omega, \omega, 0) = \gamma(0; 0, 0, 0)(1 + r\omega^2 + s\omega^4 + \dots) \quad (10)$$

for each of the components of  $\gamma$ . The absence of odd-powered terms comes about because  $\gamma(-\omega_\sigma; \omega_1, \omega_2, \omega_3) = \gamma(\omega_\sigma; -\omega_1, -\omega_2, -\omega_3)$ , as may be seen by explicitly writing out the permutations in the expression. In fact this is a general property of the hyperpolarizabilities in the absence of damping.<sup>4</sup> The form of the expansion will survive the averaging procedure, so that we may write<sup>11</sup>

$$R(\omega) = 3(1 + a\omega^2 + b\omega^4 + \dots) \quad (11)$$

for the monatomic gases, where the lowest excited state is well above our second-harmonic frequency in all cases considered. Indeed, to the extent that vibrational contri-

the exact result  $R(0) = 3$ . If we assume that Kleinman symmetry is generally valid, the immediate consequence is that  $R(\omega) = 3$  for all  $\omega$ . So by measuring  $R(\omega)$  we study departures from Kleinman symmetry.

It should be noted that in the special case of third-harmonic generation intrinsic permutation symmetry guarantees that

$$\chi_{zzz}^{(3)}(-3\omega; \omega, \omega, \omega) / \chi_{zxx}^{(3)}(-3\omega; \omega, \omega, \omega) = 3 \quad (6)$$

for all  $\omega$ .

The explicit relationship (for ESHG) between our chosen components of  $\chi^{(3)}$  and the underlying microscopic hyperpolarizabilities, of which they are orientational averages, is given by<sup>3,18</sup>

$$\chi_{zzz}^{(3)} = (\rho/90)(2\gamma_{\xi\xi\eta\eta} + \gamma_{\xi\eta\xi\xi}), \quad (7)$$

$$\chi_{zxx}^{(3)} = (\rho/90)(2\gamma_{\xi\eta\eta\xi} - \gamma_{\xi\xi\eta\eta}), \quad (8)$$

where repeated Greek indices are summed over. From this it is possible to see directly that if Kleinman symmetry holds microscopically, then  $R(\omega) = 3$ , and conversely that deviations from 3 imply that Kleinman symmetry is being violated at the microscopic level. For a closed-shell atom the averaging process is superfluous and there are only two independent components of  $\gamma$  as well as of  $\chi^{(3)}$ .

An explicit quantum-mechanical expression for  $\gamma$ , appropriate when damping may be ignored, and suitable for use even in the static limit, has been derived by Orr and Ward<sup>19</sup> and is given here:

Contributions may be ignored, the same should hold true for the molecules. This point will be discussed in greater detail below.

### III. EXPERIMENTAL PROCEDURE

The experimental apparatus is similar to that previously described by Shelton and Buckingham.<sup>20</sup> A cw laser beam is weakly focused through a gas sample subjected to a static electric field. The static field breaks the symmetry of the system, permitting the coherent generation of frequency-doubled photons. The process is intrinsically weak, but the signal is enhanced by means of periodic phase matching. This is accomplished by the use of an array of electrodes which is designed so as to reverse the polarity of the electric field every coherence length  $l_c = \pi / (2k_\omega - k_{2\omega})$ , where  $k_\omega$  is the wave vector at frequency  $\omega$  in the gas. The resulting periodic phase shift in the generated second harmonic serves to periodically cancel the accumulating phase shift due to normal dispersion, thus allowing the continued growth of the signal throughout the length of the sample. The coherence

length of the gas is adjusted to match the fixed spacing of the electrodes by varying the density of the gas until peak signal is achieved.

A schematic diagram of the experimental apparatus is shown in Fig. 1. The laser is either a cw argon-ion laser operating at 488.0 or 514.5 nm, or a dye laser pumped by the argon-ion laser and operating at 590.0 nm. The laser output is typically 1 W. The beam is redirected and its polarization is rotated by mirrors. Then a well-defined horizontal linear polarization state of the laser beam is selected by a Glan-laser prism polarizer. This is followed by a Soleil-Babinet compensator (Special Optics model No. 8-400) employed as a polarization rotating device. A filter eliminates unwanted second-harmonic light generated in the crystal quartz elements of the compensator. The beam is weakly focused, with confocal parameter about 20 cm, at the center of the electrode array (150 pairs of wires, 1.59 mm diameter and 2.69 mm center-to-center spacing, giving a horizontal field). Weak focusing is dictated by the requirement that the laser beam pass unobstructed through the long and narrow gap between the electrodes. Phase matching for this array typically occurs at a gas pressure of about 1 atm ( $T=22^\circ\text{C}$ ), except for helium (a low-dispersion medium) where the pressure is of order 100 atm. The applied field is typically 3 kV/mm, adjusted to be safely below breakdown. After transmission through the array and sample cell, the beam is recollimated and sent through a double prism spectrometer which eliminates most of the visible fundamental while passing the ultraviolet second harmonic. The Brewster angle dispersing prisms pass light polarized in the horizontal plane with negligible attenuation. A final filter eliminates the residual fundamental. The second harmonic is detected by photon counting with an uncooled EMI model No. 9893QB/350 photomultiplier tube. The dark count rate is about 1 Hz and this is usually the only background. The background is eliminated by modulating the high voltage applied to the electrodes with a square wave at 10 Hz and subtracting the voltage-off counts from the voltage-on counts. The signal is typically 1000 Hz when the pump polarization is parallel to the static field (range 50–30 000

Hz).

When the fundamental beam is polarized either parallel or perpendicular to the static field direction, the measured second-harmonic signals are

$$S_{\parallel}^{(2\omega)} \propto [\chi_{zzz}(-2\omega; \omega, \omega, 0)]^2, \quad (12)$$

or

$$S_{\perp}^{(2\omega)} \propto [\chi_{xxz}(-2\omega; \omega, \omega, 0)]^2, \quad (13)$$

respectively. In either case the second-harmonic beam will be polarized parallel to the static electric field. Therefore, the desired ratio,  $R_{\text{theor}} = \chi_{zzz} / \chi_{xxz}$ , is in principle simply determined by measuring  $R_{\text{expt}} = (S_{\parallel} / S_{\perp})^{1/2}$  since all extraneous experimental factors, such as the detection efficiency and polarization selectivity of the spectrometer, cancel out. In practice this is not necessarily so, and the main experimental problem is to track down and eliminate the various sources of systematic errors. A brief discussion follows for each of the important systematic-error sources.

The first requirement is that one prepare the fundamental beam in either of two accurately perpendicular linear polarization states. A Soleil-Babinet compensator in a fixed orientation (optic axis at  $\pi/4$  rad from the input polarization direction) was used to rotate the fundamental beam polarization by varying the compensator retardation in increments of  $\lambda/2$ . The output polarization states were tested using a second prism polarizer and found to be linearly polarized (extinction ratio  $r < 3 \times 10^{-5}$ ) and accurately orthogonal (to within 1 mrad), contributing a negligible error to  $R$ . In order that the polarization state of the laser beam not be degraded before entering the sample, care was taken to reduce the strain birefringence of the windows of the gas cell. The windows were supported on optically flat mounts at normal incidence to the beam. With only the first window in place,  $r$  was measured to be  $< 3 \times 10^{-5}$ , while with both windows in place and cycling the cell to 120 atm, the extinction ratio stayed below  $2 \times 10^{-4}$ . Modeling the input window as a wave plate with arbitrary orientation and a small phase retardation, it

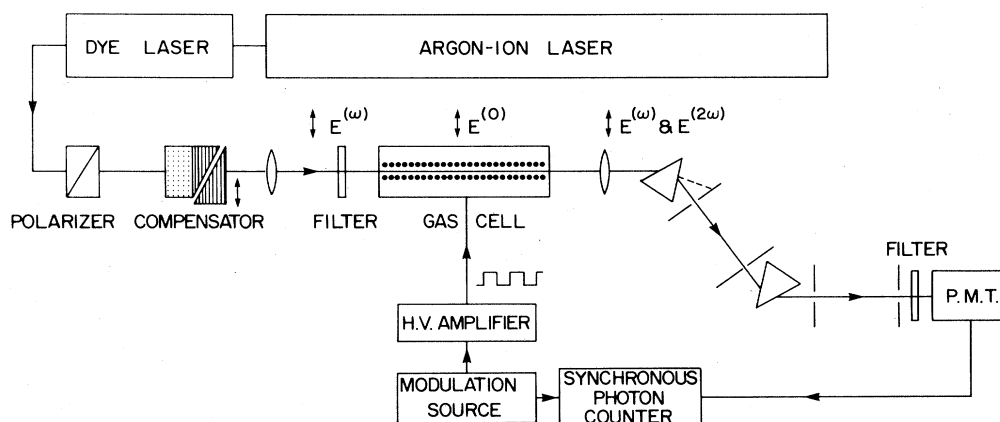


FIG. 1. Schematic diagram of the experimental apparatus showing the laser beam polarization optics, the sample cell in which the modulated ESHG beam is produced, the double Brewster angle prism spectrometer which separates the second-harmonic beam, and the electronics for synchronous photon counting. The case where the optical field polarization is parallel to the static field is illustrated. Further details are given in the text.

may be shown that the fractional increase in the measured value of  $R$  is  $2r$ , where  $r$  is the extinction ratio (the coefficient is weakly dependent on the polarization selectivity of the spectrometer and  $R \sim 3$  has been assumed). The birefringence of the optics following the input window contributes only to higher order and may be neglected. Thus, the worst-case error due to window birefringence is  $< 0.05\%$  (barring fortuitous cancellation effects).

It is necessary to align one of the polarization states parallel to the static field direction. Let the signal generated by the fundamental polarized at  $\theta$  from the horizontal be denoted as  $S_\theta$ . If the static electric field deviates from the horizontal direction by a small angle  $\delta$ , then (assuming  $R=3$ )

$$S_0/S_{\pi/2} = R^2(1 - 4\delta^2), \quad (14)$$

$$S_{\pi/3}/S_{-\pi/3} = (1 - 5\delta). \quad (15)$$

To set the electric field direction accurately parallel to the horizontal optical polarization, the cell was rotated so as to make  $S_{\pi/3} = S_{-\pi/3}$ . It was straightforward to reduce  $\delta$  to less than 5 mrad, such that resulting error in  $R$ , being quadratic in  $\delta$ , was negligible. The polarization selectivity of the spectrometer weakly affects the coefficients of the above expressions, but has no significant effect on the accuracy of the alignment which may be obtained.

In the process of preparing the fundamental beam in the desired polarization states, its intensity and direction should not be altered. By passing the input beam through the fixed plates of the compensator first and then through the movable wedge, for the ideal compensator it follows that the angles between the polarization vectors and the optic axes of the plates will be constants for each interface of every plate, for each retardation setting used ( $0$ ,  $\frac{1}{2}\lambda$ , and  $1\lambda$ ). In this case, there will be no polarization dependence of the compensator transmission. Direct measurement shows no significant polarization dependence of the transmitted intensity ( $\Delta I/I < 10^{-3}$ ). Furthermore, there will be no polarization-dependent steering of the beam in the ideal case. The residual polarization-dependent beam steering, between  $0$  or  $1\lambda$  and  $\frac{1}{2}\lambda$  retardation, was measured to be  $8 \pm 2 \mu\text{rad}$ . This beam steering of the fundamental and the collinearly generated second-harmonic beams will lead to large systematic errors in  $R$  ( $> 1\%$ ) if the second-harmonic beam is partially blocked. Careful alignment and sufficiently large collimating apertures in the spectrometer are essential to ensure unobstructed passage of the second-harmonic beam.

So far only geometric factors have been considered. The measured value of  $R$  is also sensitive to the detection nonlinearity due to dead time since  $S_{\parallel}^{(2\omega)}$  and  $S_{\perp}^{(2\omega)}$  differ by nearly an order of magnitude. The dead-time correction for the photon-counting system was made negligible by using fast electronics (pulse pair resolution 15 ns). High-purity gases were used in the experiments, though sample purity was in fact only a minor consideration. Since  $R \sim 3$  (within 10%) for all the gases studied, the effect of as much as 1% of impurities would usually be negligible. The overall stability of the apparatus was such that the measurement precision was usually limited by photon-counting statistics.

The final systematic-error source which was discovered arises if there is even a small amount of extraneous coherent second harmonic, generated outside the sample, which may interfere with the desired signal. As the quartz elements of the compensator generate such a spurious signal, a filter is used to reduce its intensity to a small fraction of the photomultiplier dark count rate, and modulation coupled with synchronous detection is used to subtract out the residual background intensity. However, because this residual background is coherent, the observed signal will be given by

$$S_{\text{obs}} \propto (E_s^2 + 2E_s E_b \cos\phi + E_b^2), \quad (16)$$

where  $E_s$  and  $E_b$  are the signal and background wave amplitudes and  $\phi$  is the relative phase shift between the two waves. In order that the cross term in the above expression be negligible (relative size  $< 10^{-3}$ ) we require that  $(E_b/E_s)^2 < 10^{-6}$ . Given the typical signal  $S_{\perp} = 100$  Hz, this indicates that a coherent background intensity of  $10^{-4}$  Hz will result in a significant systematic error. Such a small intensity is ordinarily undetectable. Fortunately, the amplitude of the ESHG wave  $E_s$  is proportional to the applied static field and changes sign when the static field does. Reversing the polarity of the static field will change the sign of the cross term in  $S_{\text{obs}}$ . Averaging results obtained before and after reversing the static field polarity will cancel out the background interference term. The interference term is clearly observed by reducing the attenuation of the presample filter and may in the future be exploited as a means of raising a very weak signal above the background to allow its shot noise limited detection.

#### IV. RESULTS

The results obtained for 15 atoms and molecules at three different wavelengths are displayed in Table I and Fig. 2, grouped according to molecular symmetry. The quoted accuracy is a factor of 10 better than the best previous results.<sup>11,12</sup> Our results (extrapolated to 694.3 nm) are consistent with the previous results. The values of  $R$  were obtained from between 3 and 15 separate runs (each involving several measurements of  $S_{\parallel}$  and  $S_{\perp}$  for positive and negative polarity of the cell voltage). The results for Xe, which were obtained at only two wavelengths, are possibly less reliable due to a slight modification of the experimental procedure.

Especially careful measurements were made for He and Ar in order that the frequency dependence of  $R(\omega)$  for these atoms could serve as a check for systematic errors (a change in the fundamental frequency necessitates changes in most of the operating parameters of the experiment). Since both the fundamental and second-harmonic frequencies involved are far below any resonance in these systems,  $R(\omega)$  must be a smooth function which extrapolates to 3 in the static limit. Our results bear this out and are consistent with the total systematic errors being less than 0.1%. The errors which we have reported are statistical estimates.

The main features of the data are the following. The measured deviations from  $R=3$  (Kleinman symmetry) are less than 2%, except for the diatomic molecules where

TABLE I. Measured deviations from Kleinman symmetry, which appear as deviations from 3 of the ratio  $R = \chi_{zzz}^{(3)}(-2\omega; \omega, \omega, 0) / \chi_{zzz}^{(3)}(-2\omega; \omega, \omega, 0)$ .

Molecule	Point group	Elements <sup>a</sup>		R		
		w	w/o	590.0 nm	Wavelength 514.5 nm	488.0 nm
He	Sphere	1	2	2.967(3)	2.952(3)	2.949(3)
Ar				2.999(3)	2.999(3)	3.000(6)
Kr				3.003(10)	3.019(3)	3.018(6)
Xe					3.034(13)	3.043(19)
CH <sub>4</sub>	T <sub>d</sub>	2	3	2.982(5)	2.977(4)	2.976(5)
CF <sub>4</sub>				2.995(13)	2.995(4)	2.999(5)
SF <sub>6</sub>				3.002(7)	3.012(4)	3.012(6)
H <sub>2</sub>	D <sub>∞h</sub>	3	7	2.890(4)	2.867(2)	2.858(3)
D <sub>2</sub>				2.909(6)	2.881(3)	2.872(4)
N <sub>2</sub>				2.951(5)	2.945(3)	2.942(4)
O <sub>2</sub>				3.126(10)	3.195(3)	3.244(6)
CO <sub>2</sub>	C <sub>3v</sub>	4	10	3.014(9)	3.025(5)	3.034(7)
C <sub>2</sub> H <sub>6</sub>				3.004(7)	3.006(3)	3.013(5)
CHF <sub>3</sub> <sup>b</sup>				2.949(7)	2.940(4)	2.925(4)
C <sub>2</sub> H <sub>4</sub>				2.957(7)	2.949(4)	2.940(6)

<sup>a</sup>The number of independent components of  $\gamma$  for ESHG, with or without Kleinman symmetry.<sup>3,21</sup>

<sup>b</sup>For CHF<sub>3</sub> both  $\beta$  and  $\gamma$  contribute in a temperature-dependent fashion (Refs. 3, 18, and 20); the measurements were made at 22 °C.

the deviations fall within the range  $\pm 8\%$ . A one-parameter fit of the form  $R(\omega) = 3[1 + A(\omega/\omega_0)^2]$  is an adequate description of the data, except for the diatomic molecules where a two-parameter fit of the form  $R(\omega) = 3[1 + A(\omega/\omega_0)^2 + B(\omega/\omega_0)^4]$  is required [see Eq. (11)]. Part of the reason for this difference may simply be that the deviations for the diatomics are much larger compared to the experimental uncertainties, thereby unmasking departures from the simpler fitting function which may also be present but unresolved for the other systems. The slope of the line fitting  $R(\omega)$  versus  $\omega$  for the atoms He, Ar, Kr, and Xe follows a regular progression with increasing size of the atom [Fig. 2(a)]. The spherical-top molecules CH<sub>4</sub>, CF<sub>4</sub>, and SF<sub>6</sub> follow the same progression [Fig. 2(b)]. The values of  $R(\omega)$  for H<sub>2</sub> and D<sub>2</sub> are significantly different [Fig. 2(c)].

Two of the molecules studied should be treated as special cases: O<sub>2</sub> and CHF<sub>3</sub>. The exceptionally large deviations observed for O<sub>2</sub> may be related to the collision-induced triplet  $\rightarrow$  singlet vibronic transitions which fall on either side of each of the laser frequencies employed. While these transitions are not dipole allowed, they have been observed in absorption<sup>22</sup> and may be important here. Further measurements should resolve this question. On the other hand, CHF<sub>3</sub> has a permanent dipole moment  $\mu^{(0)}$  which is partially oriented in the static field allowing the dominant contribution to the nonlinear susceptibility to come from the nonvanishing first hyperpolarizability  $\beta$  of the molecule. The nonlinear susceptibility, which now includes contributions from components of  $\mu^{(0)}$  and  $\beta$ , is still a fourth-rank tensor and the general results given above continue to hold.<sup>3,18,20</sup> In any case, nothing particularly distinctive occurs for CHF<sub>3</sub> with regard to Kleinman symmetry.

Vibrational resonances will occur at frequencies below the laser frequencies in this experiment, so for the molecules the behavior of  $R(\omega)$  near  $\omega=0$  will not be as sim-

ple as the fitted curves suggest. This point will be discussed in greater detail below.

## V. DISCUSSION

To see whether a simplified model might adequately account for the general features of the experimental results we considered two simple models where the dispersion of  $\chi^{(3)}$  is described in terms of a single effective resonance frequency for the system. In what follows, the effective resonance frequency of each system,  $\omega_0$ , is selected to give the best fit of the linear susceptibility to an approximate expression of the form  $\chi(\omega) \propto [1 + (\omega/\omega_0)^2]$ .<sup>23</sup>

Owyoung<sup>17</sup> has modeled isotropic systems with a classical anharmonic oscillator containing a single resonant frequency and with an anharmonic term which leaves the model suitably invariant under all symmetry transformations. The result is

$$\chi_{ijkl}^{(3)}(-\omega_\sigma; \omega_1, \omega_2, \omega_3) \propto \chi(\omega_\sigma)\chi(\omega_1)\chi(\omega_2)\chi(\omega_3) \times (\delta_{ij}\delta_{kl} + \delta_{ik}\delta_{jl} + \delta_{il}\delta_{jk}). \quad (17)$$

Note the similarity to Miller's rule.<sup>24</sup> This leads to  $\chi^{(3)}(-2\omega; \omega, \omega, 0) \propto [1 + 6(\omega/\omega_0)^2]$ . Since Kleinman symmetry is automatically satisfied by this model, it is not suitable for investigating the deviations which occur.

A more sophisticated model is given by Ward *et al.*<sup>11,25</sup> and is based on a means of estimating the dispersion in  $\chi^{(3)}(-3\omega; \omega, \omega, \omega)$  due to Dawes.<sup>26</sup> By making an effective frequency approximation in the formal expression for the hyperpolarizability [Eq. (9)] and using some exact sum rules, they obtain the result

$$\chi_{zzz}^{(3)}(-2\omega; \omega, \omega, 0) = \chi_{zzz}^{(3)}(0; 0, 0, 0) [1 + 10(\omega/\omega_0)^2 + 63(\omega/\omega_0)^4 + \dots]. \quad (18)$$

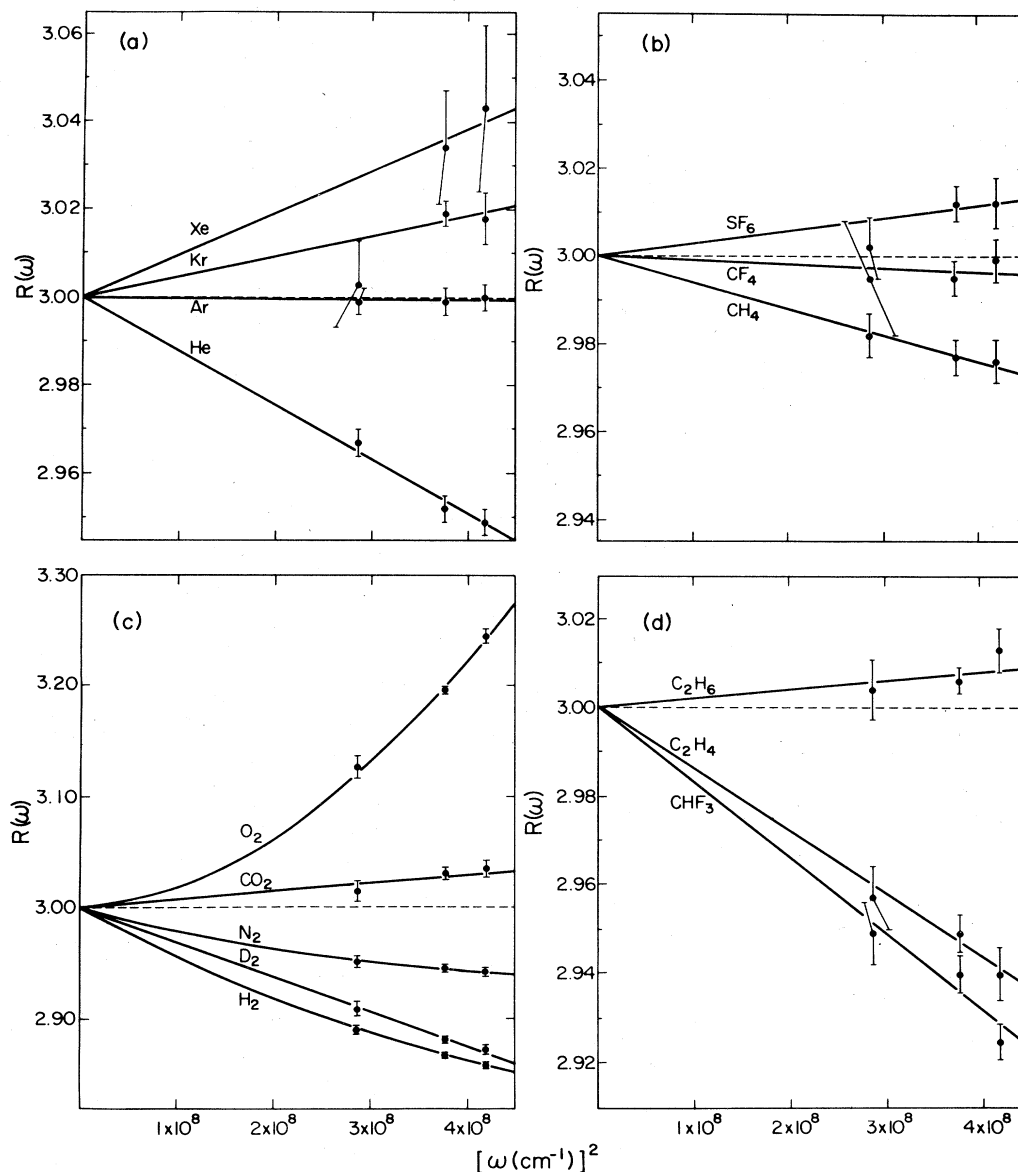


FIG. 2. Experimentally measured values of the ratio  $R(\omega) = \chi_{zzz}^{(3)} / \chi_{zzxz}^{(3)}$  are plotted as functions of  $\omega^2$ . Deviations from Kleinman symmetry correspond to deviations from  $R(\omega) = 3$  (the dashed horizontal line). The results have been grouped into the following classes: (a) inert gas atoms, (b) spherical top molecules, (c) linear molecules, and (d) nonspherical top molecules. The data are well described by straight lines constrained to pass through  $R(0) = 3$ , except for the diatomic molecules  $H_2$ ,  $N_2$ , and  $O_2$ , which require a two-parameter fit (the fitting functions and parameters are given in Table II). The deviations from Kleinman symmetry fall in the same range for all the systems studied, except the diatomic molecules where the deviations are about four times larger [note the different vertical scale in (c)].

This may be compared with the results of an *ab initio* calculation for He,<sup>27</sup> thought to be good to about 1%.<sup>28</sup> The *ab initio* results for He are adequately represented at low frequencies by

$$\chi_{zzz}^{(3)}(-2\omega; \omega, \omega, 0) = \chi_{zzz}^{(3)}(0; 0, 0, 0) [1 + 12(\omega/\omega_0)^2]. \quad (19)$$

For  $H_2$  one may combine the zero-frequency result of an *ab initio* calculation<sup>29</sup> with the result of a measurement at  $\lambda = 514.5$  nm,<sup>20</sup> to estimate the dispersion as  $[1 + 11(\omega/\omega_0)^2]$ . Thus, the model appears adequate to

describe the dispersion of  $\chi^{(3)}$  in the frequency range being considered  $[(\omega/\omega_0)^2 \sim 0.02]$ .

Taking their calculation further to include  $\chi_{zzxz}^{(3)}$ , Bigio and Ward give the result<sup>11</sup>

$$R(\omega) = 3 \left[ 1 + \frac{7}{2} (\omega/\omega_0)^2 + \dots \right]. \quad (20)$$

In order to compare this result with our measurements, we have fitted the experimental data with a function of the same form, but with an adjustable parameter  $A$  replacing the coefficient  $+7/2$  of the model. The failure of

the model is apparent upon inspection of Table II. The coefficient  $A$  is seen to have either sign, with the largest deviations being negative, in clear disagreement with the model. Furthermore, even the largest coefficients are only half as large as predicted by the model, and most of the coefficients are less than  $\frac{1}{10}$  as large.

The simple models are unable to account for either the size or the observed diversity in the deviations from Kleinman symmetry for individual systems. The problem is that there is an almost exact cancellation of the dispersion coefficients of  $\chi_{zzz}^{(3)}$  and  $\chi_{zzx}^{(3)}$  [which appear in the ratio  $R(\omega)$ ], so that the deviations from Kleinman symmetry can be 2 orders of magnitude smaller than the dispersion of the individual components of  $\chi^{(3)}$ . Calculation of Kleinman-symmetry deviations therefore requires much greater accuracy than that needed for the calculation of the dispersion of the individual components. Indeed the deviations as expressed through the formal expressions [Eq. (9)] appear to arise from a delicate interplay between terms, as dispersion upsets the balance which exists at  $\omega=0$ . It seems essential to include detailed information about the system to obtain adequate results. For these reasons the large and accurately measured deviations for He, H<sub>2</sub>, and D<sub>2</sub> should provide an important test of *ab initio* calculations for these systems.

The small deviation of the ratio  $R(\omega)$  from 3 has a clear-cut microscopic interpretation for the atoms—all the tensor components scale together to a very good approximation in the presence of dispersion. For the molecular gases one can in principle measure only two observables, and, as may be seen from Table I, there are always more than two independent microscopic components. In this case, the small size of the observed deviations tells one only that those components which were degenerate at  $\omega=0$  will remain nearly so in the presence of dispersion. There is a further complication in the case of the mole-

TABLE II. Measured dispersion coefficients for deviations from Kleinman symmetry. The data of Table I has been fitted (weighted least squares) to a one-parameter function of the form  $R(\omega)=3[1+A(\omega/\omega_0)^2]$ , except for the diatomic molecules where an additional term  $B(\omega/\omega_0)^4$  is required (see Fig. 2).

Molecule	$\omega_0^a$ ( $10^3 \text{ cm}^{-1}$ )	$A$	$B$
He	206	$-1.73 \pm 0.07$	
Ar	138	$-0.02 \pm 0.04$	
Kr	120	$+0.23 \pm 0.03$	
Xe	101	$+0.32 \pm 0.09$	
CH <sub>4</sub>	115	$-0.27 \pm 0.03$	
CF <sub>4</sub>	159	$-0.08 \pm 0.07$	
SF <sub>6</sub>	167	$+0.26 \pm 0.08$	
H <sub>2</sub>	113	$-2.04 \pm 0.19$	$+18.3 \pm 6.3$
D <sub>2</sub>	138	$-1.98 \pm 0.03$	
N <sub>2</sub>	126	$-1.22 \pm 0.32$	$+18.3 \pm 12.6$
O <sub>2</sub>	119	$+0.28 \pm 0.42$	$+80.4 \pm 17.6$
CO <sub>2</sub>	127	$+0.38 \pm 0.06$	
C <sub>2</sub> H <sub>6</sub>	115	$+0.09 \pm 0.03$	
CHF <sub>3</sub>	143	$-1.16 \pm 0.04$	
C <sub>2</sub> H <sub>4</sub>	96	$-0.43 \pm 0.02$	

<sup>a</sup>Single effective resonance frequency, from refractive index data of Ref. 30.

cules. Vibrational resonances will occur at frequencies below the incident frequency, while the dispersion expressions we have given are based on the assumption that one is far below all resonances. We will explore the consequences of these vibrational resonances in the case of H<sub>2</sub>.

First we rewrite the formal expression for  $\gamma_{\alpha\beta\gamma\delta}$  so as to explicitly display both the electronic and vibrational degrees of freedom. For a homonuclear diatomic molecule the only nonvanishing dipole matrix elements are those where the electronic quantum number changes, so the expression becomes

$$\begin{aligned} & \gamma_{\alpha\beta\gamma\delta}(-\omega_\sigma; \omega_1, \omega_2, \omega_3) \\ &= (1/\hbar^3) \sum_P \left[ \sum_{e_1, e_2, e_3 (\neq e_0)} \sum_{v_1, v_2, v_3} \frac{\langle e_0 v_0 | \mu_\alpha | e_1 v_1 \rangle \langle e_1 v_1 | \mu_\delta | e_2 v_2 \rangle \langle e_2 v_2 | \mu_\gamma | e_3 v_3 \rangle \langle e_3 v_3 | \mu_\beta | e_0 v_0 \rangle}{(\omega_{e_1 v_1, e_0 v_0} - \omega_\sigma)(\omega_{e_2 v_2, e_0 v_0} - \omega_1 - \omega_2)(\omega_{e_3 v_3, e_0 v_0} - \omega_1)} \right. \\ & \quad - \sum_{e_1, e_2 (\neq e_0)} \sum_{v_1, v_2} \frac{\langle e_0 v_0 | \mu_\alpha | e_1 v_1 \rangle \langle e_1 v_1 | \mu_\delta | e_0 v_0 \rangle \langle e_0 v_0 | \mu_\gamma | e_2 v_2 \rangle \langle e_2 v_2 | \mu_\beta | e_0 v_0 \rangle}{(\omega_{e_1 v_1, e_0 v_0} - \omega_\sigma)(\omega_{e_2 v_2, e_0 v_0} - \omega_1)(\omega_{e_2 v_2, e_0 v_0} + \omega_2)} \\ & \quad \left. + \sum_{e_1, e_3 (\neq e_0)} \sum_{v_1, v_3} \sum_{v_2 (\neq v_0)} \frac{\langle e_0 v_0 | \mu_\alpha | e_1 v_1 \rangle \langle e_1 v_1 | \mu_\delta | e_0 v_2 \rangle \langle e_0 v_2 | \mu_\gamma | e_3 v_3 \rangle \langle e_3 v_3 | \mu_\beta | e_0 v_0 \rangle}{(\omega_{e_1 v_1, e_0 v_0} - \omega_\sigma)(\omega_{e_0 v_2, e_0 v_0} - \omega_1 - \omega_2)(\omega_{e_3 v_3, e_0 v_0} - \omega_1)} \right], \quad (21) \end{aligned}$$

where  $e$  is an electronic quantum number and  $v$  is a vibrational quantum number. An explicit representation of the matrix elements would now include an integration over the internuclear coordinate. The first and last terms of this expression correspond to the first term of Eq. (9). The first two terms contain contributions coming only

from excited electronic manifolds and will be far below resonance for both the fundamental and the second harmonic of the incident light for a molecule such as H<sub>2</sub>. It is only through the last term that the excited vibrational states of the ground electronic manifold can contribute. Were the fundamental to coincide with a vibrational over-

tone then only this term would display resonant behavior, analogous to that observed in CARS spectroscopy.<sup>31,32</sup> The first two terms taken together will be rather loosely referred to as the electronic contribution and the last term as the vibrational contribution, where  $\gamma = \gamma^{\text{elec}} + \gamma^{\text{vib}}$ .

Our aim is to gauge the relative importance of the vibrational contribution. Considering only the last term we note that only the middle factor in the denominator of this term can be resonant. In the first and last factors the

field frequencies are always well below resonance regardless of the permutations considered. Hence we will ignore optical frequencies when they occur in the first or last factors in the denominator, which amounts to ignoring dispersion in the nonresonant parts of this term. This is the key approximation, which becomes exact in the static limit. Explicitly writing out the permutations we have, for example,

$$\gamma_{zzz}^{\text{vib}}(-2\omega; \omega, \omega, 0) = (1/\hbar) \sum_{v (\neq 0)} (\alpha_{0v}^{\text{zz}})^2 \left[ \frac{2}{\omega_{v,0} - \omega} + \frac{2}{\omega_{v,0} + \omega} + \frac{1}{\omega_{v,0} - 2\omega} + \frac{1}{\omega_{v,0} + 2\omega} \right], \quad (22)$$

where now  $\omega_{v,0} = \omega_{e_0 v_2, e_0 v_0}$  and

$$\alpha_{0v}^{ij} = (2/\hbar) \sum_{e_1 (\neq e_0)} \sum_{v_1} \frac{\langle e_0 v_0 | \mu_i | e_1 v_1 \rangle \langle e_1 v_1 | \mu_j | e_0 v_2 \rangle}{\omega_{e_1 v_1, e_0 v_0}} \quad (23)$$

is essentially the static limit of the transition polarizability appearing in Raman spectroscopy.<sup>33</sup>

In total there are seven independent components of  $\gamma_{\alpha\beta\gamma\delta}(-2\omega; \omega, \omega, 0)$  for a homonuclear diatomic molecule.<sup>3</sup> After making use of Eqs. (7) and (8), the two independent components of  $\chi^{(3)}$  for the gas are given by

$$\chi_{zzz}^{(3)\text{vib}}(-2\omega; \omega, \omega, 0) = \sum_{v (\neq 0)} (\rho/90\hbar) \left[ [3(\alpha_{0v}^{\text{zz}})^2 + 8(\alpha_{0v}^{\text{xx}})^2 + 4\alpha_{0v}^{\text{xx}}\alpha_{0v}^{\text{zz}}] \frac{4\omega_{v,0}}{(\omega_{v,0}^2 - \omega^2)} + [\frac{3}{2}(\alpha_{0v}^{\text{zz}})^2 + 4(\alpha_{0v}^{\text{xx}})^2 + 2\alpha_{0v}^{\text{xx}}\alpha_{0v}^{\text{zz}}] \frac{4\omega_{v,0}}{\omega_{v,0}^2 - 4\omega^2} \right], \quad (24)$$

$$\chi_{zxx}^{(3)\text{vib}}(-2\omega; \omega, \omega, 0) = \sum_{v (\neq 0)} (\rho/90\hbar) \left[ [(\alpha_{0v}^{\text{zz}})^2 + (\alpha_{0v}^{\text{xx}})^2 - 2\alpha_{0v}^{\text{xx}}\alpha_{0v}^{\text{zz}}] \frac{4\omega_{v,0}}{(\omega_{v,0}^2 - \omega^2)} + [\frac{1}{2}(\alpha_{0v}^{\text{zz}})^2 + 3(\alpha_{0v}^{\text{xx}})^2 + 4\alpha_{0v}^{\text{xx}}\alpha_{0v}^{\text{zz}}] \frac{4\omega_{v,0}}{(\omega_{v,0}^2 - 4\omega^2)} \right], \quad (25)$$

where we have taken advantage of the symmetry of the molecule to set  $\alpha^{\text{xz}} = \alpha^{\text{xy}} = 0$ ,  $\alpha^{\text{xx}} = \alpha^{\text{yy}}$  and where  $\alpha^{\text{zz}}$  and  $\alpha^{\text{xx}}$  are calculated in the principal axis system of the molecule.<sup>34</sup> In the static limit (where our result is exact) the vibrational term itself obeys the condition  $R_{\text{vib}} = \chi_{zzz}^{(3)\text{vib}}/\chi_{zxx}^{(3)\text{vib}} \rightarrow 3$  as  $\omega \rightarrow 0$ . This is true term by term in the sum over vibrational levels  $v$  and, since  $R(0) = 3$ , must be true for the electronic background as well. Furthermore, a similar calculation for the process of third-harmonic generation yields  $R_{\text{vib}} = 3$  for all  $\omega$ , in agreement with Eq. (6), indicating that our approximation retains the essential features of the problem.

Consider first the  $v=0 \rightarrow v=1$  transition. Ford and Browne<sup>35</sup> have made an *ab initio* calculation for  $\text{H}_2$ , from which we may extract the values of  $\alpha_{01}^{\text{zz}}$  and  $\alpha_{01}^{\text{xx}}$ . Although their results are averaged over the rotational levels at 300 K, whereas our expression would properly require the averaging to be done after the insertion of the  $\alpha$ , the difference is unimportant as the  $\alpha$  are slowly varying over the well-populated rotational levels. Also, their results are

strictly for the  $Q$  branch ( $\Delta J = 0$ ) transitions. There also exist  $\Delta J = \pm 2$  transitions which we will ignore as they are much weaker. Inserting the values  $\alpha_{01}^{\text{zz}} = 1.89 \times 10^{-41} \text{ C}^2 \text{ m}^2 \text{ J}^{-1}$  and  $\alpha_{01}^{\text{xx}} = 8.83 \times 10^{-42} \text{ C}^2 \text{ m}^2 \text{ J}^{-1}$  and using  $\omega_{1,0} = 4155 \text{ cm}^{-1}$  for the fundamental vibrational frequency of  $\text{H}_2$ ,<sup>31</sup> at  $\omega = 19430 \text{ cm}^{-1}$  (corresponding to  $\lambda = 514.5 \text{ nm}$ ) we obtain

$$\chi_{zzz}^{(3)\text{vib}} = (-4.1 \times 10^{-64} \text{ C}^4 \text{ m}^4 \text{ J}^{-3}) \rho / 6, \quad (26)$$

$$\chi_{zxx}^{(3)\text{vib}} = (-5.6 \times 10^{-65} \text{ C}^4 \text{ m}^4 \text{ J}^{-3}) \rho / 6. \quad (27)$$

We have not included the contributions from higher vibrational overtones. The next largest contribution will come from the  $v=0 \rightarrow v=2$  transition. Its size may be estimated by using the available results from an *ab initio* calculation for the isotropically averaged  $\langle \alpha_{0v}^{ij} \rangle$ .<sup>36</sup> Since the  $v=0 \rightarrow v=2$  susceptibility will be related to the  $v=0 \rightarrow v=1$  susceptibility by a factor of order  $(\langle \alpha_{02} \rangle / \langle \alpha_{01} \rangle)^2 = 0.01$ , and the higher overtones give even smaller contributions, one may safely ignore them.



The above results may be compared with the experimentally measured value for  $\chi_{zzz}^{(3)}(-2\omega; \omega, \omega, 0)$  at  $\lambda = 514.5$  nm for  $H_2$ ,<sup>20</sup>

$$\chi_{zzz}^{(3)} = (5.71 \pm 0.06 \times 10^{-62} \text{ C}^4 \text{ m}^4 \text{ J}^{-3}) \rho / 6 \quad (28)$$

(the experimental uncertainty is dominated by the uncertainty of the He *ab initio* calculation used for calibration). Further, from the *ab initio* calculation of Jaszunski and Roos<sup>29</sup> one may (by isotropically averaging) derive the zero frequency value of

$$\chi_{zzz}^{(3)}(0; 0, 0, 0) = (4.31 \times 10^{-62} \text{ C}^4 \text{ m}^4 \text{ J}^{-3}) \rho / 6. \quad (29)$$

Since their calculation includes vibrations only by averaging  $\gamma$  over internuclear coordinates of the vibronic ground state, the overtones of the ground electronic manifold are not included.<sup>37</sup> Therefore the above value may be identified with our  $\chi^{(3)\text{elec}}$ .

By choosing the simplest form for the dispersion of  $\chi^{(3)\text{elec}}$  we obtain

$$R(\omega) = \frac{\chi_{zzz}^{\text{elec}}(0; 0, 0, 0)(1 + a\omega^2) + \chi_{zzz}^{\text{vib}}(-2\omega; \omega, \omega, 0)}{\frac{1}{3}\chi_{zzz}^{\text{elec}}(0; 0, 0, 0)(1 + b\omega^2) + \chi_{zzz}^{\text{vib}}(-2\omega; \omega, \omega, 0)}. \quad (30)$$

From our calculated values of  $\chi^{(3)\text{vib}}$ , the *ab initio* result for  $\chi_{zzz}^{\text{elec}}(0; 0, 0, 0)$ , the measured value of  $\chi_{zzz}^{(3)}$  at  $\lambda = 514.5$  nm, and the measured value of  $R(\omega)$  at  $\lambda = 514.5$  nm, this expression allows us to predict  $R(\omega)$  for any other frequency. The results are shown in Fig. 3, along with the curve obtained by setting  $\chi^{(3)\text{vib}} = 0$  in the above expression. In view of the approximations made, the agreement with the experimental values is satisfactory. The effect of the vibrational resonance at  $4155 \text{ cm}^{-1}$  is to reduce the value of  $R(\omega)$  in the region of our measurements, and at  $\lambda = 514.5$  nm this model predicts that the resonance contributes about 10% of the total deviation. It has been suggested that vibrational contributions to ESHG in the visible are insignificant.<sup>25</sup> Our results are in accord with this assessment for  $\chi^{(3)}$ , but  $R(\omega)$  is such a sensitive function of  $\chi^{(3)}$  that we cannot, in our case, dismiss the role of vibrations. Furthermore, our calculations indicate that  $\chi_{zzz}^{(3)\text{vib}}$  contributes about 20% of the total  $\chi_{zzz}^{(3)}$  for  $H_2$  at  $\omega = 0$ . [This follows from Eqs. (24) and (29).]

The deviations from Kleinman symmetry for  $H_2$  and  $D_2$  differ by about 10%, and one may ask whether this difference is accounted for by vibrational resonances. While we do not have sufficient information to model  $D_2$

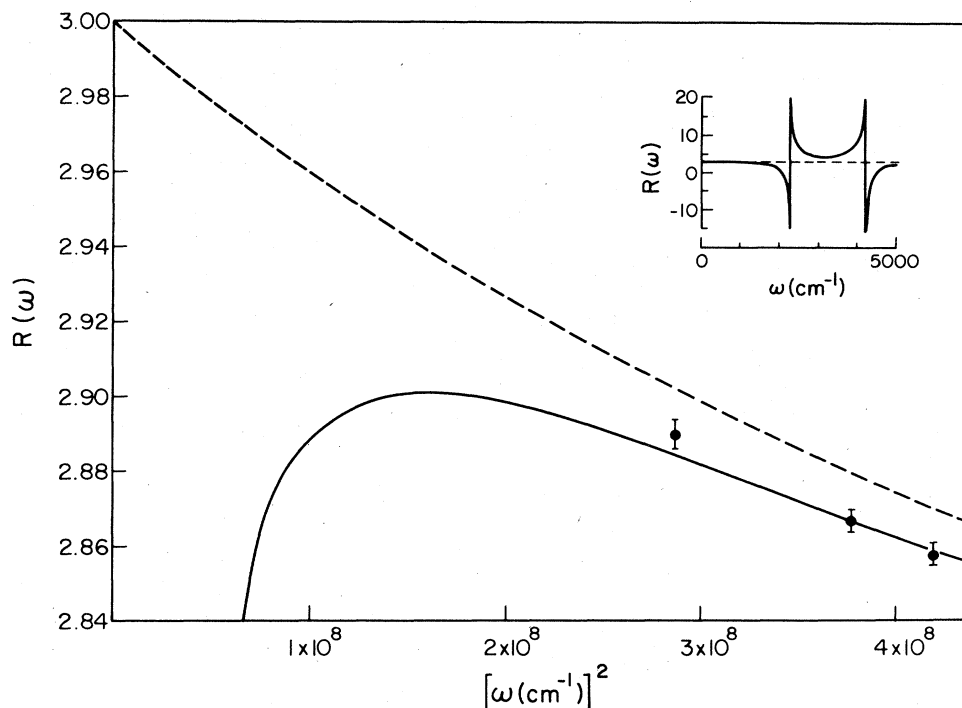


FIG. 3. Measured and calculated  $R(\omega)$  vs  $\omega^2$  are compared for  $H_2$ . The solid curve includes both the electronic and the vibrational resonance contributions, while the dashed curve shows the calculated results when the vibrational contribution is switched off. The calculation has been constrained to match the experimental  $R(\omega)$  at one point ( $\lambda = 514.5$  nm). In the frequency range of the experimental measurements the effect of the vibrational resonances is to shift the curve by a small amount with little change in shape, while at lower frequencies the vibrations dominate. The inset shows the calculated  $R(\omega)$  in the region of the  $v = 0 \rightarrow v = 1$  vibrational transition of  $H_2$ . The two peaks correspond to one- and two-photon resonance terms (the peak frequencies are shifted up by 51 and  $232 \text{ cm}^{-1}$  from  $\omega_{01}$  and  $\omega_{01}/2$ ). The large downward excursion in the main figure corresponds to the high-frequency tail of the resonances shown in the inset. The second overtone ( $\Delta v = 2$ ) is negligible for frequencies more than a few hundred  $\text{cm}^{-1}$  from resonance, and higher overtones are negligible outside even smaller ranges.

as we have modeled  $H_2$ , it seems likely that the first overtone for  $D_2$  is of comparable strength to that of  $H_2$ . In that case, the vibrational shifts in  $R(\omega)$  will be about the same for  $H_2$  and  $D_2$ . If so, then the 10% difference in the deviations of  $H_2$  and  $D_2$  must come largely from differences in their electronic terms. In fact what we have called the electronic term contains some of the vibrational nature of the molecule as expressed through the matrix elements, whose explicit representation requires an integration over the internuclear coordinates. For this reason even the linear polarizabilities of  $H_2$  and  $D_2$  differ by about 1%.<sup>38,39</sup> On the other hand, the low-lying vibrational resonances play no role in the linear polarizability for a homonuclear diatomic molecule.

Finally, we note that although a link has been made in the literature<sup>8</sup> between the Born-Oppenheimer approximation and Kleinman symmetry, our results, in particular for the inert gases, do not bear this out.

## VI. CONCLUSION

The frequency dependence of the observed deviations from Kleinman symmetry is in qualitative agreement with that expected on general grounds, but simple models cannot account for the deviations in a quantitative fashion. The measured deviations should provide a sensitive test of the accuracy of *ab initio* calculations, especially for the simplest systems ( $He$ ,  $H_2$ , and  $D_2$ ). In the frequency region studied the deviations appear to be mainly electronic in origin. At lower frequencies, and at  $\omega=0$  in particular, our calculations indicate that vibrations will make a substantial contribution to the total hyperpolarizability of a molecule.

## ACKNOWLEDGMENTS

This work was supported by grants from the Natural Sciences and Engineering Research Council (NSERC) of Canada and from the Research Corporation (New York).

- <sup>1</sup>Y. R. Shen, *Principles of Nonlinear Optics*, (Wiley, New York, 1984).
- <sup>2</sup>D. C. Hanna and M. A. Yuratich, *Nonlinear Optics of Free Atoms and Molecules* (Springer, Berlin, 1979).
- <sup>3</sup>M. P. Bogaard and B. J. Orr, in *International Review of Science, Physical Chemistry, Molecular Structure and Properties*, edited by A. D. Buckingham (Butterworths, London, 1975), Ser. 2, Vol. 2, p. 149.
- <sup>4</sup>P. N. Butcher, *Nonlinear Optical Phenomena Bulletin 200*, Engineering Experimental Station (Ohio State University, Columbus, Ohio, 1965).
- <sup>5</sup>D. A. Kleinman, *Phys. Rev.* **126**, 1977 (1962).
- <sup>6</sup>N. Bloembergen, *Nonlinear Optics*, (Benjamin, New York, 1965).
- <sup>7</sup>P. A. Franken and J. F. Ward, *Rev. Mod. Phys.* **35**, 23 (1963).
- <sup>8</sup>R. W. Hellwarth, *Prog. Quantum Electron.* **5**, 1 (1977).
- <sup>9</sup>M. Okada and S. Ieiri, *Phys. Lett.* **34A**, 63 (1971).
- <sup>10</sup>F. Zernike and P. R. Berman, *Phys. Rev. Lett.* **15**, 999 (1965).
- <sup>11</sup>I. J. Bigio and J. F. Ward, *Phys. Rev. A* **9**, 35 (1974).
- <sup>12</sup>J. F. Ward and I. J. Bigio, *Phys. Rev. A* **11**, 60 (1975).
- <sup>13</sup>C. K. Miller and J. F. Ward, *Phys. Rev. A* **16**, 1179 (1977).
- <sup>14</sup>P. S. Pershan, *Phys. Rev.* **130**, 919 (1963).
- <sup>15</sup>A. D. Buckingham and B. J. Orr, *Chem. Soc. London Q. Rev.* **21**, 195 (1967).
- <sup>16</sup>H. Jeffreys, *Cartesian Tensors* (Cambridge University, Cambridge, 1963).
- <sup>17</sup>A. Owyong, Ph.D. thesis, California Institute of Technology, 1972.
- <sup>18</sup>S. Kielich, *IEEE J. Quantum Electron.* **QE-5**, 562 (1969).
- <sup>19</sup>B. J. Orr and J. F. Ward, *Mol. Phys.* **20**, 513 (1971).
- <sup>20</sup>D. P. Shelton and A. D. Buckingham, *Phys. Rev. A* **26**, 2787 (1982).
- <sup>21</sup>A. D. Buckingham, in *Advances in Chemical Physics, Intermolecular Forces*, Vol. XII, edited by J. O. Hirschfelder (Interscience, 1967).
- <sup>22</sup>G. C. Tabisz, E. J. Allin, and H. L. Welsh, *Can. J. Phys.* **47**, 2859 (1969).
- <sup>23</sup>M. Born and E. Wolf, *Principles of Optics* (Pergamon, Oxford, 1980).
- <sup>24</sup>R. C. Miller, *Appl. Phys. Lett.* **5**, 17 (1964).
- <sup>25</sup>D. S. Elliott and J. F. Ward, *Mol. Phys.* **51**, 45 (1984).
- <sup>26</sup>E. L. Dawes, *Phys. Rev.* **169**, 47 (1968).
- <sup>27</sup>P. Sitz and R. Yaris, *J. Chem. Phys.* **49**, 3546 (1968).
- <sup>28</sup>R. Klingbeil, *Phys. Rev. A* **7**, 48 (1973).
- <sup>29</sup>M. Jaszunski and B. O. Roos, *Mol. Phys.* **52**, 1209 (1984).
- <sup>30</sup>Landolt-Bornstein, *Zahlenwerte und Funktionen*, Band II, Teil 8 (Springer, Berlin, 1962).
- <sup>31</sup>F. Moya, S. A. J. Druet, and J. P. E. Taran, *Opt. Commun.* **13**, 169 (1975).
- <sup>32</sup>W. M. Huo and R. L. Jaffe, *Phys. Rev. Lett.* **47**, 30 (1981).
- <sup>33</sup>M. Born and K. Huang, *Dynamical Theory of Crystal Lattices*, (Clarendon, Oxford, 1954).
- <sup>34</sup>S. J. Cyvin, J. E. Rauch, and J. C. Decius, *J. Chem. Phys.* **43**, 4083 (1965).
- <sup>35</sup>A. L. Ford and J. C. Browne, *Phys. Rev. A* **7**, 418 (1973).
- <sup>36</sup>J. D. Poll, in *Planetary Atmospheres*, International Astronomical Union Symposium No. 40, edited by C. Sagan *et al.* (Reidel, Dordrecht, 1971) p. 384.
- <sup>37</sup>D. M. Bishop and L. M. Cheung, *J. Chem. Phys.* **72**, 5125 (1980).
- <sup>38</sup>J. Rychlewski, *J. Chem. Phys.* **78**, 7252 (1983).
- <sup>39</sup>K. Kołos and L. Wolniewicz, *J. Chem. Phys.* **46**, 1426 (1967).